Monotopic Enzymes and Lipid Bilayers: A Comparative Study†

Philip W. Fowler,‡,§,|| Kia Balali-Mood,‡,|| Sundeep Deol,‡ Peter V. Coveney,§ and Mark S. P. Sansom*,‡

Department of Biochemistry, University of Oxford, South Parks Road, Oxford OX1 3QU, U.K., and Centre for Computational Science, Department of Chemistry, University College London, 20 Gordon Street, London WC1H 0AJ, U.K.

Received December 4, 2006; Revised Manuscript Received January 16, 2007

ABSTRACT: Monotopic proteins make up a class of membrane proteins that bind tightly to, but do not span, cell membranes. We examine and compare how two monotopic proteins, monoamine oxidase B (MAO-B) and cyclooxygenase-2 (COX-2), interact with a phospholipid bilayer using molecular dynamics simulations. Both enzymes form between three and seven hydrogen bonds with the bilayer in our simulations with basic side chains accounting for the majority of these interactions. By analyzing lipid order parameters, we show that, to a first approximation, COX-2 disrupts only the upper leaflet of the bilayer. In contrast, the top and bottom halves of the lipid tails surrounding MAO-B are more and less ordered, respectively, than in the absence of the protein. Finally, we identify which residues are important in binding individual phospholipids by counting the number and type of lipid atoms that come close to each amino acid residue. The existing models that explain how these proteins bind to bilayers were proposed following inspection of the X-ray crystallographic structures. Our results support these models and suggest that basic residues contribute significantly to the binding of these monotopic proteins to bilayers through the formation of hydrogen bonds with phospholipids.

Unlike globular proteins, integral membrane proteins (IMPs)[1] usually possess extended hydrophobic surfaces. These interact with the fatty acyl chains of phospholipids, thereby helping to bind the protein to the membrane. IMPs were classified by Blobel (*1*) into three broad groupings: polytopic, bitopic, and monotopic. Polytopic proteins traverse the membrane more than once; bitopic proteins cross the membrane only once, and monotopic proteins interact with only one leaflet of the bilayer.

Despite the fact that they do not span the membrane, there are only a few structures of monotopic proteins compared to polytopic proteins. This explains in part our relatively poor understanding of how these proteins attach themselves to membranes. Picot et al. (*2*) reported the first structure of a monotopic protein in 1994. This was of the first isozyme of prostaglandin H2 synthase (PGHS) which, due to its cyclooxygenase function, is more commonly known as COX-1. Structures of the second isozyme of PGHS, known as COX-2, quickly followed (*3*−*7*). More recently, structures of squalene hopene cyclase (*8*, *9*), monoamine oxidase B (MAO-B) (*10*, *11*), and fatty acid amide hydrolase (*12*) have been reported. All four of these monotopic proteins are important targets for pharmacological intervention, and all have hydrophobic substrates.

MAO-B and COX-2 are suggested to bind to phospholipid bilayers in somewhat different ways (see Figure 1). Binda et al. (*10*) hypothesized that each MAO-B monomer is attached to a bilayer by several hydrophobic patches and a single transmembrane (TM) helix. By contrast, Picot et al. (*2*) suggested that COX-1 and COX-2 associate with the upper leaflet of the membrane via three short amphipathic α-helices, known as the membrane-binding domain. These helices lie parallel to the membrane−water interface and allow the protein to "float" on the surface of the bilayer.

The aim of this paper is to study and compare how MAO-B and COX-2 interact with a phospholipid bilayer. We have used molecular dynamics (MD) simulations, an established computational technique (*13*−*18*), to evolve the dynamics of both MAO-B and COX-2 in phospholipid bilayers. MD simulations enable us to extrapolate from static X-ray structures to a more dynamic picture of membrane proteins (*18*, *19*) and in particular to identify the key interactions lipids make with these proteins (*20*). Studies of this kind will therefore complement the growing body of experimental literature that seeks to understand how lipids interact with membrane proteins (*21*, *22*). Although a number of reports of peptides at the phospholipid bilayer interface have been published (*23*, *24*), there have been comparatively few computational studies of membrane-bound monotopic proteins (*19*, *25*). We therefore decided to examine two different monotopic proteins so that we may compare their behavior.

Eukaryotic MAO catalyzes the oxidative deamination of primary and secondary aromatic amines to imines. Mammalian MAO exists in two isoforms, called MAO-A and

† This work was supported by grants from BBSRC, EPSRC, and the Wellcome Trust. We are grateful to the UK National Grid Service for allowing us access to their computer nodes. P.W.F. thanks EPSRC for funding his Ph.D. and the Wellcome Trust for further support. K.B.-M. thanks BBSRC for funding.

* To whom correspondence should be addressed. E-mail: mark.sansom@bioch.ox.ac.uk. Telephone: +44 1865 275 371. Fax: ++44 1865 275 273.

‡ University of Oxford.

§ University College London.

|| These authors contributed equally to this work.

[1] Abbreviations: IMP, integral membrane protein; MAO, monoamine oxidase; COX, cyclooxygenase; PGHS, prostaglandin H2 synthase; POPC, palmitoyloleoylphosphatidylcholine; POPE, palmitoyloleoylphosphatidylethanolamine; FAD, flavin adenine dinucleotide; rmsd, root-mean-square deviation; MD, molecular dynamics; TM, transmembrane.

10.1021/bi602455n CCC: $37.00
Published on Web 02/21/2007

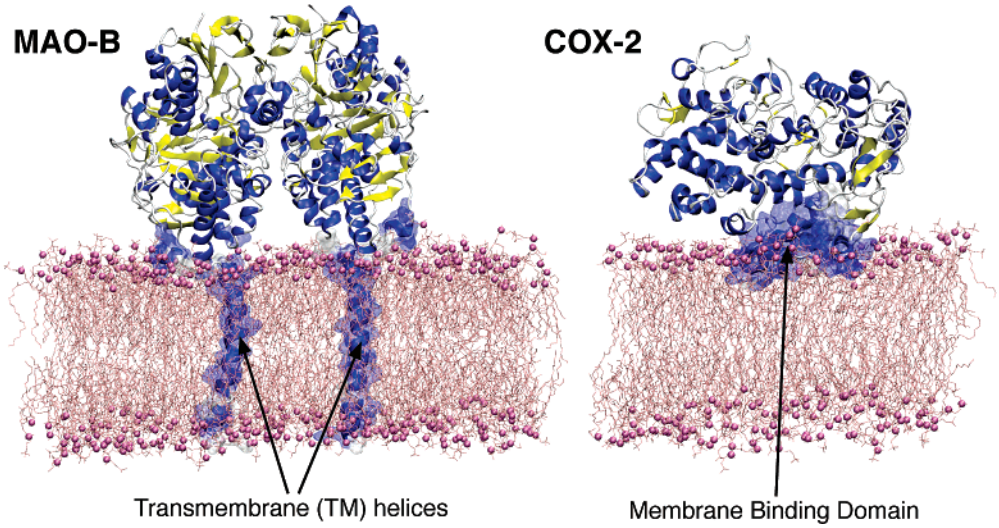

FIGURE 1: Attachment of MAO-B and COX-2 to membranes. The TM helices of MAO-B anchor the protein to the phospholipid bilayer, whereas COX-2 interacts with the phospholipid bilayer using a membrane-binding domain composed of three α-helices. Both these pictures are snapshots from the molecular dynamics simulations. α-Helices are colored dark blue and *β*-sheets yellow, and the phospholipid bilayer without hydrogens is colored pink. The phosphate groups of the lipids have been drawn as pink spheres to help identify the interface between the bilayer and the solvent. For clarity, no waters are shown.

MAO-B, and each is encoded by a separate gene (*26*). MAO is primarily located on the outer mitochondrial membrane in neural tissues (*27*, *28*), and it has been implicated in a number of neurological illnesses, for example, depression (*29*, *30*). MAO-B binds phenylethylamine, benzylamine, and dopamine (*29*).

Prostaglandin H2 synthase (COX) catalyzes the conversion of arachidonic acid, a 20-carbon fatty acid, to prostaglandin H2, the precursor of the prostaglandin class of local hormones (*31*). Prostaglandins mediate a variety of crucial physiological processes, such as the aggregation of platelets. Two isoforms of COX have been elucidated thus far (COX-1 and COX-2). COX-1 is constitutively expressed and is mainly involved in maintaining physiological homeostasis, for example, maintaining the mucosal lining of the stomach (*31*). COX-2 is induced, and rat models have demonstrated that this enzyme is involved in the local pain and inflammation responses (*32*, *33*). Nonsteroidal anti-inflammatory drugs, such as aspirin and ibuprofen, bind to and inhibit both isoforms of COX and are the primary pharmacological means of alleviating pain and reducing inflammation.

METHODS

Initial conformations for both proteins were derived from the appropriate high-resolution X-ray crystallographic structures (PDB entries 1OJA for human MAO-B and 5COX for mouse COX-2) (*6*, *11*). The sequence numbering in this paper reflects that of the original structural papers. A list of which molecular dynamics codes and force fields were used is given in Table 1. GROMACS[2] (*34*−*36*) in combination with the GROMOS96 force field (*37*) was used to simulate the dynamics of MAO-B, and NAMD2[3] (*38*, *39*) in combination with the CHARMM27 force field (*40*) was used to simulate COX-2.

Both enzymes are homodimers and are approximately the same size. However, due to our use of the more detailed CHARMM force field, we decided to model only the monomer of COX-2 to reduce the amount of computer time needed. Only parts of the TM helices of MAO-B were resolved in the X-ray crystallographic structure. Residues 497−520 and 502−520 were unresolved for the first and second MAO-B monomer, respectively. We hypothesized that these residues completed the TM α-helix; this was supported by the results of a transmembrane helix prediction tool (*41*). The missing residues were then modeled by assuming the helix extends across the whole membrane.

Table 1: Summary of the Simulations

simulation	no. of residues per monomer	no. of atoms	molecular dynamics package	force field
MAO-B dimer	518	374 047	GROMACS-3.1.4	GROMOS96
COX−2 monomer	556	101 815	NAMD2.5	CHARMM27

Table 2: Details of the Simulation Unit Cells

	MAO-B	COX-2
POPC	654	197
POPE	478	0
waters	100860	22163
counterions	4 Cl^-	5 Na^+
cofactors	2 FAD	1 heme

Table 2 lists how many of each type of molecule is present in each simulation unit cell. MAO-B was inserted into a pre-equilibrated bilayer of palmitoyloleoylphosphatidylethanolamine (POPE) and palmitoyloleoylphosphatidylcholine (POPC) in a ratio of 3:4; this mixture is a reasonable approximation of the mitochondrial outer membrane. There is less POPE in the membrane of the endoplasmic reticulum, and therefore, COX-2 was inserted into a simple POPC bilayer. Counterions were added to ensure that both simulation unit cells were electrically neutral. Last, the cofactors flavine adenine dinucleotide (FAD) and heme were included in the MAO-B and COX-2 simulation unit cells, respectively. We shall now turn our attention to the setup and simula-

[2] From http://www.gromacs.org.
[3] From http://www.ks.uiuc.edu/research/namd.

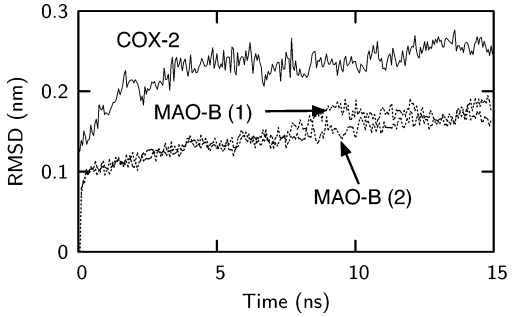

FIGURE 2: Conformations of both MAO-B and COX-2 do not change significantly over the course of the molecular dynamics simulations as measured by the root-mean-square deviation (rmsd) of the C_α atoms when compared to their respective X-ray crystallographic structures. A dimer of MAO-B was modeled, and therefore, the rmsd for each monomer, excluding the transmembrane (TM) helix, is plotted and labeled.

tion of the MAO-B simulation unit cell as the details for COX-2 have been described previously (*19*).

All electrostatic forces were calculated using the particle mesh Ewald method (*42*, *43*). van der Waals interactions were computed for all pairs of atoms separated by no more than 1.0 nm. The lengths of all bonds were constrained using the LINCS algorithm (*44*), permitting an integration time step of 2 fs to be used. The dynamics of the MAO-B simulation unit cell were evolved for 15 ns. The protein was simulated in the isobaric−isothermal (NPT) ensemble, and a constant pressure of 1 bar was applied independently in all directions using a Parrinello-Rahman barostat (*45*) using a pressure coupling constant of 5.0 ps. Water, lipid, and protein were coupled separately to Nosé-Hoover thermostats at 300 K with a temperature coupling constant of 1.0 ps (*46*, *47*). All analysis of the MD trajectories was performed using either the GROMACS suite of analysis programs or VMD (*48*).

RESULTS

We shall first assess the conformational stability of our membrane-bound MAO-B and COX-2 models before examining how integrated each protein is into its bilayer and whether the bilayer has been perturbed. Finally, we shall investigate which MAO-B and COX-2 residues form interactions with the phospholipid bilayer.

Conformational Stability. The root-mean-square deviation (rmsd) of the backbone C_α atoms of a protein provides a measure of conformational drift during a simulation (Figure 2). The rmsd values for both MAO-B and COX-2 initially rapidly increase relative to their X-ray crystallographic structures. The rmsd values for COX-2 reach an approximate plateau after ~5 ns and then fluctuate between 0.20 and 0.28 nm. This indicates that during the first 5 ns of the simulation the protein is equilibrating and settling into the bilayer (*19*). Since there are two MAO-B monomers, we may calculate the rmsd for each. The TM helix is excluded as the outer domains move slightly relative to the TM helix, increasing the rmsd values by up to 0.05 nm (data not shown). The rmsd values for both MAO-B monomers are very similar and are less than 0.20 nm. As the monomers of both proteins are similar in size, this indicates that the structure of COX-2 is more flexible than the structure of MAO-B while bound

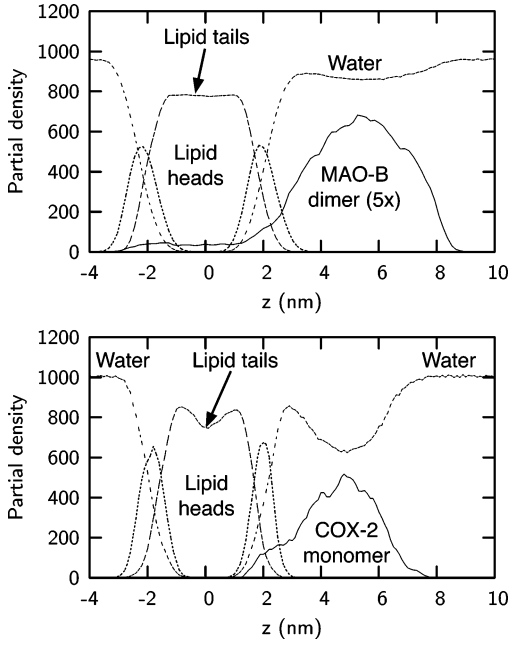

FIGURE 3: Partial densities along an axis, *z*, perpendicular to the membrane averaged over the last 5 ns of each simulation. This shows that the interface between the phospholipid bilayer and solvent extends over 2−3 nm. The partial density of MAO-B has been multiplied by 5 to show that it extends all the way across the membrane, whereas the partial density of the COX-2 monomer shows that it penetrates only into the top leaflet of the membrane. All densities are measured in kilograms per cubic meter.

to the membrane. This could be due to the relative stability of each protein's fold or the differing method of attachment to the membrane or might indicate that the COX-2 dimer would be more stable. Despite the rmsd values for both MAO-B monomers remaining below 0.2 nm for the entire simulation, we shall be conservative and assume that the structure of MAO-B takes 10 ns to relax. For the remainder of our analysis, we shall therefore consider the last 5 ns of each 15 ns simulation.

Protein Location Relative to the Bilayer. To investigate how well each protein is integrated into the bilayer, we compute the partial density for the protein, the water, and the lipid tails and headgroups as a function of an axis, *z*, perpendicular to the membrane for the last 5 ns of each simulation (Figure 3). The partial density of MAO-B persists across the entire membrane, whereas the partial density of COX-2 indicates that it interacts only with the upper leaflet and the membrane-binding domain rarely penetrates to a level deeper than that defined by the lipid headgroups.

Bilayer Perturbations. To investigate the degree to which the proteins perturb the hydrophobic core of their bilayers, we compute the deuterium order parameter of the acyl chains (*49*).

$$S_z = \frac{3}{2}\langle \cos^2 \theta_z \rangle - \frac{1}{2}$$

where S_z is the order parameter and θ_z is the angle between the *z*-axis and the molecular axis under consideration. This last axis is defined as the vector from C_{n-1} to C_{n+1}, when C_n is a specific carbon in the acyl chains. The order parameters for the palmitoyl chains are plotted in Figure 4. As expected, the presence of COX-2 significantly disrupts the upper leaflet

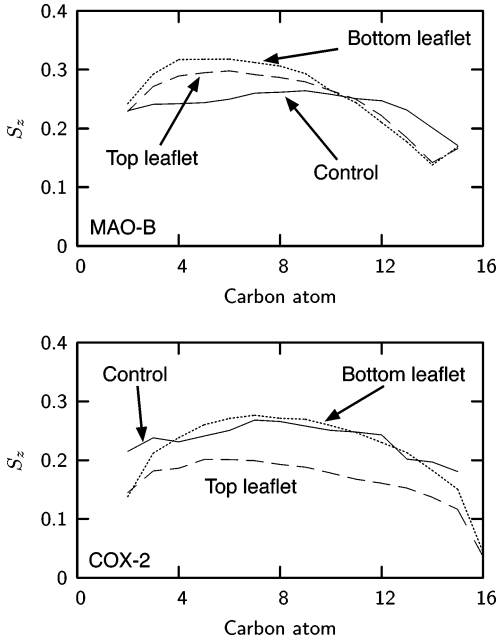

FIGURE 4: Deuterium order parameters for the palmitoyl chains of the upper and lower leaflets for both the MAO-B and COX-2 simulations. A control for the appropriate unperturbed membrane is plotted, and where the calculated order parameter is lower than the control, the lipids are less ordered at that carbon atom.

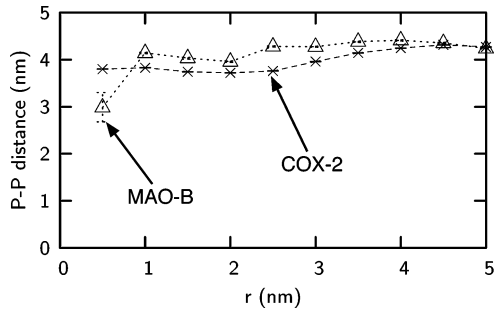

FIGURE 5: The bilayer is thinner around both proteins as shown by how the separation between the phosphorus atoms of lipids in the top and bottom leaflets varies with the distance from the geometrical center of the each monotopic protein. In all cases, error bars are plotted but are often smaller than the symbols.

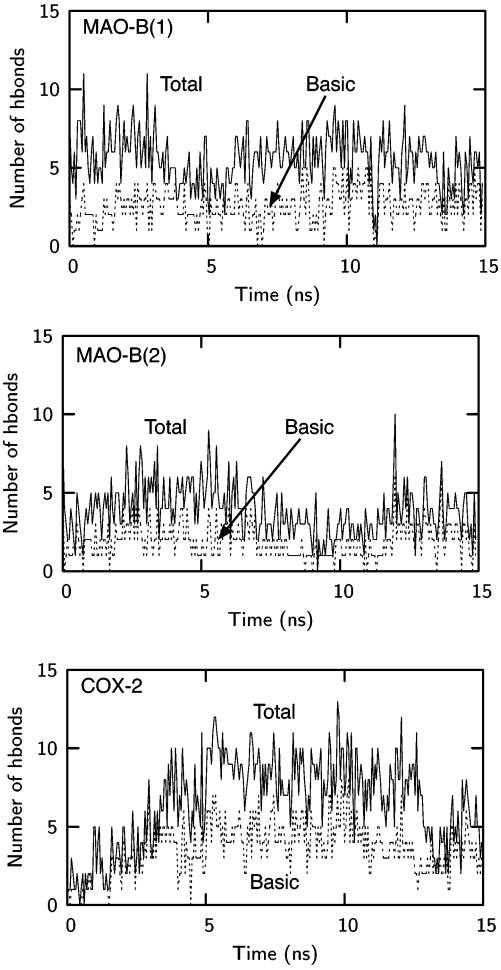

FIGURE 6: Total number (approximately three to seven) of hydrogen bonds formed between the phospholipids and either of the two MAO-B monomers or COX-2. Basic residues (Arg and Lys) are especially proficient at forming hydrogen bonds with the membrane and make up the majority of hydrogen bonds for both proteins. The difference in behavior in the first 5 ns between MAO-B and COX-2 is due to differences in how each protein was inserted into the membrane. The MAO-B monomers are labeled MAO-B(1) and MAO-B(2). A hydrogen bond is assumed to have formed if the distance between the donor and acceptor atoms is <0.35 nm and the angular deviation is $<30°$.

but disrupts the bottom leaflet only slightly. The results for MAO-B are more complex; if we divide the palmitoyl chain at C_{10} into two halves, then, for both leaflets, the upper half of the chain is more ordered and the lower half is less or equally ordered. We suggest that this is due to the lipids being forced into a more ordered configuration by the presence of the transmembrane α-helices. The splaying of the ends of the palmitoyl chains in both cases is most likely due to a slight thinning of the bilayer around the protein. This is confirmed by the variation in the average distance between the phosphorus atoms of the bilayer (Figure 5). The width of the bilayer is reduced within a radius of 2.5 nm from the geometrical center of MAO-B. The presence of COX-2 also reduces the width of the bilayer, and this effect persists up to 3.0 nm from the protein. For COX, this is consistent with the tails of phospholipids "curling" underneath the membrane-binding domain, leading to a less ordered bilayer. The number of lipids is necessarily lower near either protein, and therefore, the uncertainty in the width of the bilayer within 1 nm of the proteins is large. We cannot state which protein reduces the width of the bilayer the most since the bilayers are different. We shall now consider how the proteins interact with the phospholipids.

Protein−Lipid Interactions. The headgroups of both POPC and POPE are highly polar and can therefore form electrostatic interactions, including hydrogen bonds with both MAO-B and COX-2. We shall first investigate which protein residues form hydrogen bonds before studying in general which protein residues interact with the phospholipids.

Counting the number of hydrogen bonds as each simulation progresses (Figure 6) shows that, for the final 5 ns of each simulation, the two monomers of MAO-B form 5.2 and 3.5 hydrogen bonds and the COX-2 monomer forms 6.6 hydrogen bonds on average with the phospholipid bilayer. Further examination showed that basic residues (arginine and lysine) form the majority of these hydrogen bonds. This is intuitive since the positively charged side chains of arginine and lysine can easily form hydrogen bonds with the negatively charged phosphate group of the phospholipids. The enthalpic contribution from the formation of these

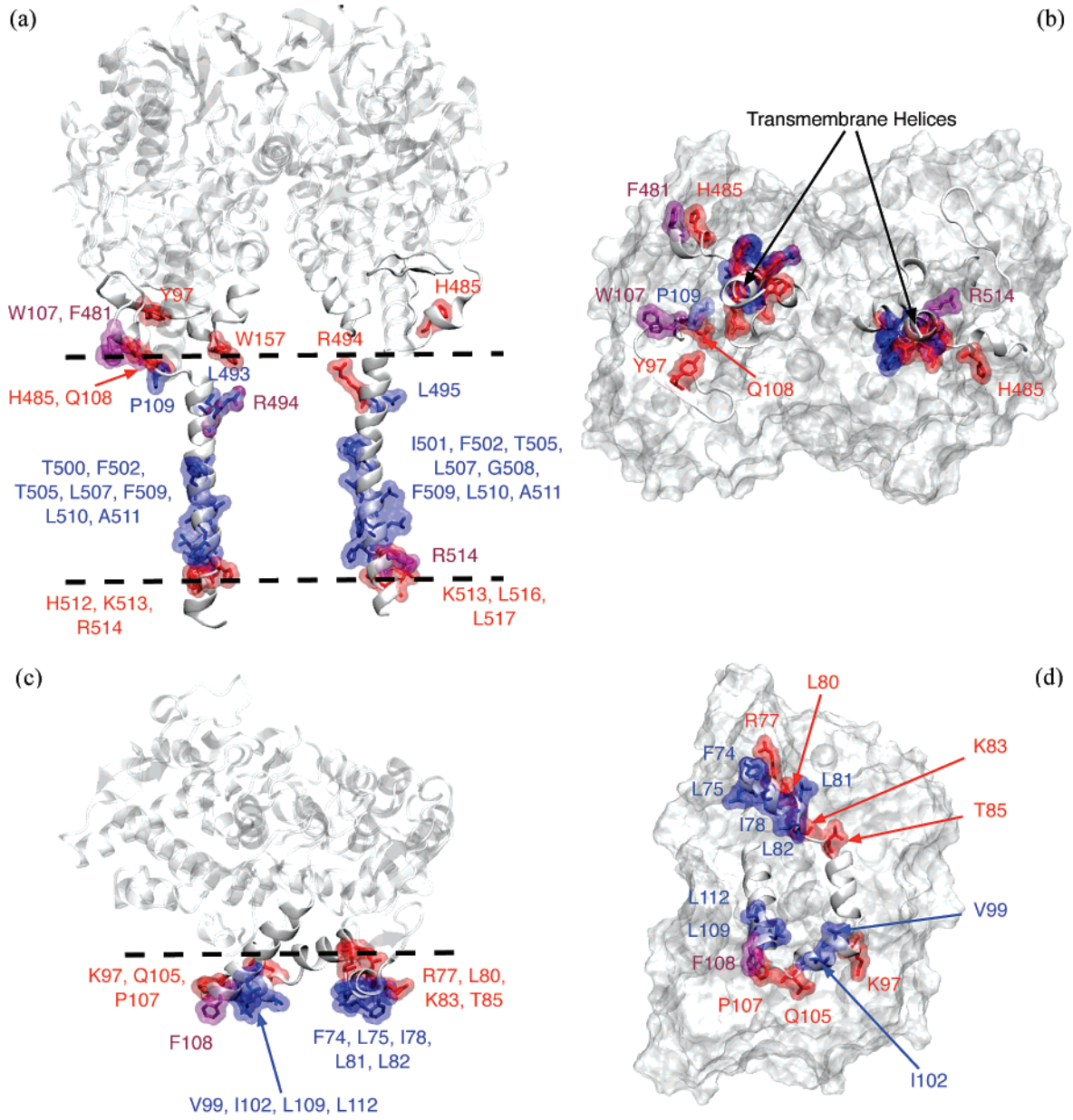

FIGURE 7: Residues of MAO-B and COX-2 that interact with phospholipids as determined by counting the average number of polar and nonpolar lipid atoms within either 0.35 nm for COX-2 or 0.45 nm for MAO-B over the last 5 ns of each simulation. The longer distance compensates for the lack of nonpolar hydrogens in the reduced atom description of MAO-B and the lipids. The side views of MAO-B and COX-2 are shown in panels a and c, respectively. Views from beneath the protein, i.e., a "membrane-eye'' perspective, are given in panels b and d for MAO-B and COX-2, respectively. For reasons of clarity, the majority of the protein is represented by a simple surface in these illustrations. Residues that significantly interact with polar and nonpolar lipid atoms are colored red and blue, respectively. The dashed line indicates the approximate center of the lipid−water interface. Note that several residues, for example, F108 of COX-2, are colored purple as these residues significantly interact with both polar and nonpolar lipid atoms.

hydrogen bonds will aid the binding of both MAO-B and COX-2 to phospholipid bilayers. It is perhaps significant that COX-2, lacking a TM "anchor", forms slightly more H-bonds with the bilayer. These observations support the proposal that basic residues play a vital role in the anchoring of monotopic proteins in membranes (*50*).

The free energy of binding of a monotopic protein to a membrane is composed of enthalpic and entropic components. We shall not investigate any entropic effects as it is unlikely that the dynamics of the protein, water, or bilayer have been adequately sampled. Instead, we shall examine which residues interact with the phospholipids. We shall do this by counting the number of polar and nonpolar atoms that are close to each residue during the last 5 ns of each simulation. We do not expect this analysis to identify all the key residues because the rearrangement of the individual phospholipids around the protein is very slow, but it is likely that we have captured the majority of those amino acid residues that are particularly important in forming interactions with individual phospholipids. We shall consider only the residues that form a significant number of interactions. These we define as those residues that account for the top half of interactions. For example, 112 residues of the MAO-B dimer are observed to come into close contact with polar atoms of a phospholipid during the 5 ns; however, only 16 residues account for 50% of these events. The residues of COX-2

display a similar skewed behavior. The residues that we identified as significant are shown in Figure 7.

As expected, the generally hydrophobic amino acids at the center of the TM helices of MAO-B (notably F502 and F509) interact with the nonpolar atoms of the phospholipids. Bracketing this band of residues are two bands of basic, polar and a few hydrophobic residues (especially W107, F481, R494, K513, and R514) that interact with the polar atoms of the phospholipids. For COX-2, we observe several hydrophobic residues (notably F74, L81, L82, I102, and F108) on the base of the membrane-binding domain pointing down into the interior of the membrane and interacting with nonpolar atoms of the phospholipids and mostly polar and basic residues (especially R77, L80, T85, K97, and Q105) pointing up or out into the membrane and interacting with polar atoms of the phospholipids. It is likely that the basic residues are forming electrostatic interactions with the phosphate groups of the lipids.

Interestingly, in both cases, we observe several residues that, according to our criteria, interact with both polar and nonpolar lipid atoms. These are F108 for COX-2 and W107, F451, R494, and R514 for MAO-B. It is likely that this is partially because these are residues with long side chains and therefore are more likely to be able to be simultaneously close to both nonpolar and polar lipid atoms and partially because of the amphipathic nature of, for example, tryptophan and phenylalanine. These aromatic amphipathic residues can readily interact with charged polar residues either by backbone hydrogen bonding or by forming π interactions with positively charged choline groups. There is strong evidence from statistical studies of existing X-ray crystallographic structures that aromatic amphipathic residues (tryptophan and tyrosine) have an important role to play at the membrane interface in stabilizing membrane proteins (*50*−*52*). It has also been noted that leucine is the most common amino acid in monotopic proteins (*50*), and we indeed observe for COX-2 six (of 17 residues) and for MAO-B eight (of 34) leucines interacting with the membrane.

If we examine the distribution of interacting residues across the MAO-B dimer in more detail, we see that the first MAO-B monomer [MAO-B(1)] interacts more closely with the membrane. This hypothesis is supported by our earlier hydrogen bond analysis which indicated that the left-hand monomer forms, on average, more hydrogen bonds during the last 5 ns of the simulations. This could, for example, be indicative of a slow rocking motion that is alternatively pushing one monomer and then the other deeper into the membrane. Substantially longer simulations, however, would be required to demonstrate this more conclusively.

DISCUSSION

We have examined how two monotopic proteins, MAO-B and COX-2, interact with a phospholipid bilayer using molecular dynamics. The structures of both proteins did not change significantly relative to their X-ray crystallographic structures. The bilayer is perturbed in different ways by the presence of either COX-2 or MAO-B. After a period during which the protein integrates into the bilayer and the phospholipids undergo a degree of rearrangement, monomers of both proteins formed on average between three and seven hydrogen bonds with individual phospholipids. Although relatively few in number, basic residues formed the majority of these hydrogen bonds. Finally, we examined which residues are likely to be important in forming enthalpic interactions with the membrane by counting the number of polar and nonpolar lipid atoms within a specified distance of each residue. We found that a small number of residues dominated the observed interactions and that, in general, polar amino acid residues interacted with polar lipid atoms and nonpolar amino acid residues interacted with nonpolar lipid atoms. There were exceptions to this rule, notably the few residues that were observed forming interactions with both polar and nonpolar lipid atoms. If we assume that the average number of lipid atoms in the proximity to a protein residue correlates with the enthalpy of binding, then this calculation indicates which residues are important for the binding of MAO-B and COX-2 to the membrane.

By examining the X-ray crystallographic structure of MAO-B, Binda et al. (*10*) suggested that, in addition to the TM helix, residues 157, 99−112, and 481−488 formed interactions with a bilayer. This hypothesis is supported by experiments which demonstrated that MAO-B remains bound to the membrane even when the TM helix is truncated by mutagenesis (*53*). Our results correspond well with these predictions. We observed residue 157 and residues within loops 99−112 and 481−488 interacting with the membrane. Picot et al. (*2*) proposed that the three α-helices formed by residues 73−116 (the membrane-binding domain) interacted with the bilayer. This mechanism was novel at the time and has been subsequently confirmed in a number of experiments (*54*, *55*). In our simulations, only residues in the membrane-binding domain of COX-2 interacted with the phospholipid bilayer, and hence, our observations support and help explain this mechanism. Our predictions for which residues are important for the attachment of both monotopic proteins to membranes may be tested by mutagenesis experiments. Although both MAO-B and COX-2 have been extensively studied using mutagenesis experiments, the majority of these have focused on mutating active site residues which are buried within the proteins (refs *56* and *57* and references cited therein). Unsurprisingly, none of these residues were observed interacting with the phospholipid bilayer. Although Spencer et al. (*54*) examined the effect of mutating groups of hydrophobic and aromatic amphipathic residues on the membrane-binding domain of COX-1, comparatively few residues were mutated, and those that were are not conserved between COX-1 and COX-2.

The substrates of MAO-B and COX-2 are predominantly hydrophobic and, we assume, are partitioned into the membrane. Both substrates possess opposing charges, and it is interesting to speculate what effect altering the charge distribution of the enzymes would have on not just the ability of the enzyme to bind to the membrane but also how strongly the enzyme binds its substrate. For example, basic residues can form hydrogen bonds and electrostatic interactions with the phosphate group of phospholipids but may decrease the affinity of MAO-B for its positively charged substrate by electrostatic repulsion. Binda et al. (*10*) suggested that the residues on loop 99−112 cover an entrance cavity leading to the active site. There is only a single arginine (R100) on this loop despite it lying at the membrane−water interface.

We hypothesize that mutating residues in this loop to arginine or lysine may increase the free energy of binding between MAO-B and the membrane but may lead to a decrease in the activity of the enzyme. In a similar vein, Binda et al. (*58*) proposed that the positive charge of the substrates of MAO would ensure that they are localized near the phosphate groups within the membrane, thereby enhancing their local concentration.

It should be recognized that there are some shortcomings in a theoretical study of this nature. First, the dynamics of both proteins were sampled for only nanoseconds. It is probable that there are motions with larger correlation times, and these would not be detected by a study of this kind (*59*). This might include more significant rearrangements of phospholipids around the proteins or motion of the proteins within the bilayer. It is possible to lessen, but not eliminate, this potential problem by extending or repeating the simulations. Running far longer simulations would also relax any artificial stresses in the bilayer introduced by the insertion of the protein into the membrane. This is a problem common to all membrane protein simulations. Second, to maximize the accuracy of the comparison between the two proteins, it is necessary to ensure that the methods that are used are identical. Unfortunately, this is not the case as both different molecular dynamics codes and force fields were used for each protein. We do not, however, expect this to significantly alter the results we describe here since we have avoided making detailed quantitative comparisons.

Last, although COX-2 exists as a dimer, only a monomer is modeled. We assume that the monomer does not behave in a manner significantly different from that of the dimer over the nanosecond time scale accessed by our simulations. It would also be interesting to examine both the effect of changing the lipid composition and, should any detailed mutagenesis information become available, how the dynamics of MAO-B or COX-2 change when such mutations are made.

REFERENCES

1. Blobel, G. (1980) Intracellular protein topogenesis, *Proc. Natl. Acad. Sci. U.S.A. 77*, 1496−1500.
2. Picot, D., Loll, P., and Garavito, R. (1994) The X-ray crystal structure of the membrane protein prostaglandin H2 synthase-1, *Nature 367*, 243−249.
3. Loll, P. J., Picot, D., and Garavito, R. M. (1995) The structural basis of aspirin activity inferred from the crystal structure of inactivated prostaglandin H2 synthase, *Nat. Struct. Biol. 2*, 637−643.
4. Gupta, K., Selinsky, B. S., Kaub, C. J., Katz, A. K., and Loll, P. J. (2004) The 2.0 Å resolution crystal structure of prostaglandin H2 synthase-1: Structural insights into an unusual peroxidase, *J. Mol. Biol*. *335*, 503−518.
5. Loll, P. J., Picot, D., Ekabo, O., and Garavito, R. M. (1996) Synthesis and use of iodinated non-steroidal antiinflammatory drug analogs as crystallographic probes of the prostaglandin H2 synthase cyclooxygenase active site, *Biochemistry 35*, 7330−7340.
6. Kurumbail, R. G., Stevens, A. M., Gierse, J. K., McDonald, J. J., Stegeman, R. A., Pak, J. Y., Gildehaus, D., Miyashiro, J. M., Penning, T. D., Seibert, K., Isakson, P. C., and Stallings, W. C. (1996) Structural basis for selective inhibition of cyclooxygenase-2 by anti-inflammatory agents, *Nature 384*, 644−648.
7. Luong, C., Miller, A., Barnett, J., Chow, J., Ramesha, C., and Browner, M. F. (1996) Flexibility of the NSAID binding site in the structure of human cyclooxygenase-2, *Nat. Struct. Biol. 3*, 927−933.
8. Wendt, K. U., Poralla, K., and Schulz, G. E. (1997) Structure and function of a squalene cyclase, *Science 277*, 1811−1815.
9. Wendt, K. U., Lenhart, A., and Schulz, G. E. (1999) The structure of the membrane protein squalene-hopene cyclase at 2.0 Å resolution, *J. Mol. Biol. 286*, 175−187.
10. Binda, C., Newton-Vinson, P., Hubálek, F., Edmondson, D. E., and Mattevi, A. (2002) Structure of human monoamine oxidase B, a drug target for the treatment of neurological disorders, *Nat. Struct. Biol. 9*, 22−26.
11. Binda, C., Li, M., Hubálek, F., Restelli, N., Edmondson, D. E., and Mattevi, A. (2003) Insights into the mode of inhibition of human mitochondrial monoamine oxidase B from high-resolution crystal structures, *Proc. Natl. Acad. Sci. U.S.A. 100*, 9750−9755.
12. Bracey, M. H., Hanson, M. A., Masuda, K. R., Stevens, R. C., and Cravatt, B. F. (2002) Structural adaptations in a membrane enzyme that terminates endocannabinoid signaling, *Science 298*, 1793−1796.
13. Daggett, V. (2006) Protein folding-simulation, *Chem. Rev. 106*, 1898−1916.
14. Saiz, L., Bandyopdhyay, S., and Klein, M. L. (2002) Towards an understanding of complex biological membranes from atomistic molecular dynamics simulations, *Biosci. Rep. 22*, 151−173.
15. Petrache, H. I., Grossfield, A., MacKenzie, K. R., Engelman, D. M., and Woolf, T. B. (2000) Modulation of glycophorin A transmembrane helix interactions by lipid bilayers: Molecular dynamics calculations, *J. Mol. Biol. 302*, 727−746.
16. Hansson, Y., Oostenbrink, C., and van Gunsteren, W. F. (2002) Molecular dynamics simulations, *Curr. Opin. Struct. Biol. 12*, 190−196.
17. Karplus, M., and McCammon, J. (2002) Molecular dynamics simulations of biomolecules, *Nat. Struct. Biol. 9*, 646−652.
18. Gumbart, J., Wang, Y., Aksimentiev, A., Tajkhorshid, E., and Schulten, K. (2005) Molecular dynamics simulations of proteins in lipid bilayers, *Curr. Opin. Struct. Biol. 15*, 423−431.
19. Fowler, P. W., and Coveney, P. V. (2006) A computational protocol for the integration of the monotopic protein prostaglandin H2 synthase into a phospholipid bilayer, *Biophys. J. 91*, 401−410.
20. Deol, S. S., Bond, P. J., Domene, C., and Sansom, M. S. (2004) Lipid-protein interactions of integral membrane proteins: A comparative simulation study, *Biophys. J. 87*, 3737−3749.
21. Lee, A. G. (2006) How lipids and proteins interact in a membrane: A molecular approach, *Mol. BioSyst. 1*, 203−212.
22. Marsh, D., and Páli, T. (2004) The protein−lipid interface: Perspectives from magnetic resonance and crystal structures, *Biochim. Biophys. Acta 1666*, 118−141.
23. Balali-Mood, K., Harroun, T. A., and Bradshaw, J. P. (2005) Membrane-bound ARF1 peptide: Interpretation of neutron diffraction data by molecular dynamics simulation methods, *Mol. Membr. Biol. 22*, 379−388.
24. Chandrasekhar, I., van Gunsteren, W. F., Zandomeneghi, G., Williamson, P. T., and Meier, B. H. (2006) Orientation and conformational preference of leucine-enkephalin at the surface of a hydrated dimyristoylphosphatidylcholine bilayer: NMR and MD simulation, *J. Am. Chem. Soc. 128*, 159−170.
25. Nina, M., Bernèche, S., and Roux, B. (2000) Anchoring of a monotopic membrane protein: The binding of prostaglandin H2 synthase-1 to the surface of a phospholipid bilayer, *Eur. Biophys. J. 29*, 439−454.
26. Bach, A. W. J., Lan, N. C., Johnson, D. L., Abell, C. W., Bembenek, M. E., Kwan, S., Seeburg, P. H., and Shih, J. C. (1988) cDNA cloning of human liver monoamine oxidase A and B: Molecular basis of differences in enzymatic properties, *Proc. Natl. Acad. Sci. U.S.A. 85*, 4934−4938.
27. Greenawalt, J. W., and Schnaitman, C. (1970) An appraisal of the use of monoamine oxidase as an enzyme marker for the outer membrane of rat liver mitochondria, *J. Cell Biol. 46*, 173−179.
28. Urban, P., Andersen, J. K., Hsu, H.-P. P., and Pompon, D. (1991) Comparative membrane locations and activities of human monoamine oxidases expressed in yeast, *FEBS Lett. 286*, 142−146.
29. Shih, J. C., Chen, K., and Ridd, M. J. (1999) Monoamine oxidase: From genes to behaviour, *Annu. Rev. Neurosci. 22*, 197−217.
30. Cesura, A. M., and Pletscher, A. (1992) The new generation of monoamine oxidase inhibitors, *Prog. Drug Res. 38*, 171−297.
31. Goetzl, E. J., An, S., and Smith, W. L. (1995) Specificity of expression and effects of eicosanoids mediators in normal physiology and human disease, *FASEB J. 9*, 1051−1058.
32. Masferrer, J. L., Zweifel, B. S., Manning, P. T., Hauser, S. D., Leahy, K. M., Smith, W. G., Isakson, P. C., and Seibert, K. (1994) Selective inhibition of inducible cyclooxygenase 2 *in vivo* is

antiinflammatory and nonulcerogenic, *Proc. Natl. Acad. Sci. U.S.A. 91*, 3228−3232.
33. Seibert, K., Zhang, Y., Leahy, K. M., Hauser, S. D., Masferrer, J. L., Perkins, W., Lee, L., and Isakson, P. C. (1994) Pharmacological and biochemical demonstration of the role of cyclooxygenase 2 in inflammation and pain, *Proc. Natl. Acad. Sci. U.S.A. 91*, 12013−12017.
34. Lindahl, E., Hess, B., and van der Spoel, D. (2001) A package for molecular simulation and trajectory analysis, *J. Mol. Model. 7*, 306−317.
35. Berendsen, H., van der Spoel, D., and van Drunen, R. (1995) GROMACS: A message-passing parallel molecular dynamics implementation, *Comput. Phys. Commun. 91*, 43−56.
36. van der Spoel, D., Lindahl, E., Hess, B., Groenhof, G., Mark, A. E., and Berendsen, H. J. (2005) GROMACS: Fast, flexible and free, *J. Comput. Chem. 26*, 1701−1718.
37. van Gunsteren, W. F., Billeter, S. R., Eising, A. A., Hunenberger, P. H., Kruger, P., Mark, A. E., Scott, W. R. P., and Tironi, I. G. (1996) *Biomolecular simulation: The GROMOS96 manual and user guide*, Hochschulverlag an der ETH/Biomos, Zurich.
38. Kalé, L., Skeel, R., Bhandarkar, M., Brunner, R., Gursoy, A., Krawetz, N., Phillips, J., Shinozaki, A., Varadarajan, K., and Schulten, K. (1999) NAMD2: Greater scalability for parallel molecular dynamics, *J. Comput. Phys. 151*, 283−312.
39. Phillips, J., Braun, R., Wang, W., Gumbart, J., Tajkhorshid, E., Villa, E., Chipot, C., Skeel, R. D., Kalé, L., and Schulten, K. (2005) Scalable molecular dynamics with NAMD, *J. Comput. Chem. 26*, 1781−1802.
40. Foloppe, N., and MacKerell, A. D., Jr. (2000) All-atom empircal force field for nucleic acids: I. Parameter optimization based on small molecule and condensed phase macromolecular target data, *J. Comput. Chem. 21*, 86−104.
41. Cuthbertson, J. M., Doyle, D. A., and Sansom, M. S. (2005) Transmembrane helix prediction: A comparative evaluation and analysis, *Protein Eng., Des. Sel. 18*, 295−308.
42. Darden, T., York, D., and Pedersen, L. (1993) Particle mesh Ewald: An N-log(N) method for Ewald sums in large systems, *J. Chem. Phys. 98*, 10089−10092.
43. Essmann, U., Perea, L., Berkowitz, M. L., Darden, T., Lee, H., and Pedersen, L. G. (1995) A smooth particle mesh Ewald method, *J. Chem. Phys. 103*, 8577−8593.
44. Hess, B., Bekker, H., Berendsen, H. J. C., and Fraaije, J. G. E. M. (1997) LINCS: A linear constraint solver for molecular simulations, *J. Comput. Chem. 18*, 1463−1472.
45. Parrinello, M., and Rahman, A. (1981) Polymorphic transitions in single crystals: A new molecular dynamics method, *J. Appl. Phys. 85*, 7182−7190.
46. Nosé, S. (1984) A molecular dynamics method for simulations in the canonical ensemble, *Mol. Phys. 52*, 255−268.
47. Hoover, W. G. (1985) Canonical dynamics: Equilibrium phase-space distributions, *Phys. Rev. A 31*, 1695−1697.
48. Humphrey, W., Dalke, A., and Schulten, K. (1996) VMD-Visual Molecular Dynamic, *J. Mol. Graphics 14*, 33−38.
49. Moraes, C. M., and Bechinger, B. (2004) Peptide-related alterations of membrane-associated water: Deuterium solid-state NMR investigations of phosphatidylcholine membranes at different hydration levels, *Magn. Reson. Chem. 42*, 155−161.
50. Granseth, E., von Heijne, G., and Elofsson, A. (2005) A study of the membrane-water interface region of membrane proteins, *J. Mol. Biol. 346*, 377−385.
51. Ulmschneider, M. B., Sansom, M. S. P., and Di Nola, A. (2005) Properties of integral membrane protein structures: Derivation of an implicit membrane potential, *Proteins 59*, 252−265.
52. Hessa, T., Kim, H., Bihlmaier, K., Lundin, C., Boekel, J., Andersson, H., Nilsson, I., White, S. H., and von Heijne, G. (2005) Recognition of transmembrane helices by the endoplasmic reticulum translocon, *Nature 433*, 377−381.
53. Rebrin, I., Geha, R. M., and Shih, J. C. (2001) Effects of Carboxyl-terminal Truncations on the Activity and Solubility of Human Monoamine Oxidase B, *J. Biol. Chem. 276*, 29499−29506.
54. Spencer, A. G., Thuresson, E., Otto, J. C., Song, I., Smith, T., DeWitt, D. L., Garavito, R. M., and Smith, W. L. (1999) The membrane binding domains of prostaglandin endoperoxide H synthases 1 and 2, *J. Biol. Chem. 274*, 32936−32942.
55. Li, Y., Smith, T., Grabski, S., and DeWitt, D. L. (1998) The membrane association sequences of the prostaglandin endoperoxide synthases-1 and -2 isozymes, *J. Biol. Chem. 273*, 29830−29837.
56. Youdim, M. B. H., Edmondson, D., and Tipton, K. F. (2006) The therapeutic potential of monoamine oxidase inhibitors, *Nat. Rev. Neurosci. 7*, 295−309.
57. Simmons, D. L., Botting, R. M., and Hla, T. (2004) Cyclooxygenase isozymes: The biology of prostaglandin synthesis and inhibition, *Pharmacol. Rev. 56*, 387−437.
58. Binda, C., Hubálek, F., Li, M., Edmondson, D. E., and Mattevi, A. (2004) Crystal structure of human monoamine oxidase B, a drug target enzyme monotopically inserted into the mitochondrial outer membrane, *FEBS Lett. 564*, 225−228.
59. Grossfield, A., Feller, S. E., and Pitman, M. C. (2007) Convergence of molecular dynamics simulations of membrane proteins, *Protein Eng. Des. Sel.*, doi:10.1002/prot.21308.

BI602455N